

# Identification and shell model calculation of high spin states in $^{137,138}\text{Cs}$ nuclei

K. Li,<sup>1</sup> Y. X. Luo,<sup>1,2</sup> J. K. Hwang,<sup>1</sup> A. V. Ramayya,<sup>1</sup> J. H. Hamilton,<sup>1</sup> S. J. Zhu,<sup>1,3</sup> C. Goodin,<sup>1</sup> H. L. Crowell,<sup>1</sup> J. O. Rasmussen,<sup>2</sup> I. Y. Lee,<sup>2</sup> S. C. Wu,<sup>2</sup> A. Covello,<sup>4</sup> A. Gargano,<sup>4</sup> R. Donangelo,<sup>5</sup> G. M. Ter-Akopian,<sup>6</sup> A. V. Daniel,<sup>6</sup> J. D. Cole,<sup>7</sup> W. C. Ma,<sup>8</sup> and M. A. Stoyer<sup>9</sup>

<sup>1</sup>Physics Department, Vanderbilt University, Nashville, Tennessee 37235, USA

<sup>2</sup>Lawrence Berkeley National Laboratory, Berkeley, California 94720, USA

<sup>3</sup>Physics Department, Tsinghua University, Beijing 100084, People's Republic of China

<sup>4</sup>Dipartimento di Scienze Fisiche, Università di Napoli Federico II, and Istituto Nazionale di Fisica Nucleare, Complesso Universitario di Monte S. Angelo, Via Cintia, 80126 Napoli, Italy

<sup>5</sup>Universidade Federal do Rio de Janeiro, CP 68528, RG Brazil

<sup>6</sup>Flerov Laboratory for Nuclear Reactions, JINR, Dubna, Russia

<sup>7</sup>Idaho National Laboratory, Bldg. IRCPL, MS2114, Idaho Falls, Idaho 83415, USA

<sup>8</sup>Mississippi State University, Drawer 5167, Mississippi State, Mississippi 39762, USA

<sup>9</sup>Lawrence Livermore National Laboratory, Livermore, California 94550, USA

(Received 21 September 2006; published 26 April 2007)

High spin states of  $^{137,138}\text{Cs}$  have been studied by measuring  $\gamma$ - $\gamma$  coincidences from the spontaneous fission of  $^{252}\text{Cf}$  with the LBNL Gammasphere detector array. The high spin level scheme of the  $N = 83$  neutron-rich Cs ( $Z = 55$ ) isotope,  $^{138}\text{Cs}$ , built on the  $6^-$  isomeric state, has been established for the first time up to a 4626 keV level, assigned  $(16^+)$ . The level scheme of  $^{137}\text{Cs}$  has been expanded up to a 5495 keV level, assigned  $(31/2^-)$ . Spins, parities, and configurations are assigned based on the agreement between experimental level energies and shell model calculations and level systematics. Similarities are observed in the  $N = 82$  isotones,  $^{137}\text{Cs}$  and  $^{135}\text{I}$ , up to  $17/2^+$  as well as in the  $N = 83$  isotones,  $^{138}\text{Cs}$  and  $^{136}\text{I}$ , up to  $12^-$ . The shell model calculations indicate the important role played by interactions between the excitation of the valence protons outside the  $Z = 50$  major shell and the  $f_{7/2}$  valence neutron outside the  $N = 82$  major shell.

DOI: [10.1103/PhysRevC.75.044314](https://doi.org/10.1103/PhysRevC.75.044314)

PACS number(s): 23.20.Lv, 21.60.Cs, 25.85.Ca, 27.60.+j

## I. INTRODUCTION

Studies of neutron-rich nuclei near the  $N = 82$  closed shell with a few protons beyond the  $Z = 50$  closed shell are of interest to test nuclear shell model calculations that utilize effective interactions. A straightforward and important question is “To what extent is the spherical shell model (SSM) valid for neutron-rich nuclei near the  $N = 82$  shell?” With one valence neutron outside the  $N = 82$  closed shell and a few valence protons beyond the  $Z = 50$  closed shell, the  $N = 83$  isotones under consideration are adjacent to the doubly magic nucleus  $^{132}\text{Sn}$ . The structure of these nuclei could provide additional understanding of the proton-neutron and proton-proton interactions and of the similarities of the structures of nuclei around  $^{132}\text{Sn}$  and  $^{208}\text{Pb}$  [1].

$\beta$  decay [2],  $(d, p)$  and  $(\alpha, xn)$  reactions [3], thermal neutron capture, and fission [2] have been used to populate the  $N = 83$  isotones. Detailed exploration of the high spin yrast and near-yrast spectroscopy in this region was not realized until the advent of large  $\gamma$ -detector arrays used in fission experiments [4,5]. Before the present work, some progress was made at the Gammasphere and Eurogam II arrays on the  $N = 83$  isotones  $^{134}\text{Sb}$  ( $Z = 51$ ) [6],  $^{135}\text{Te}$  ( $Z = 52$ ) [6–8],  $^{136}\text{I}$  ( $Z = 53$ ) [6,9,10],  $^{137}\text{Xe}$  ( $Z = 54$ ) [9,11,12], and  $^{139}\text{Ba}$  ( $Z = 56$ ) [8]. The ground state and a number of low spin states [13] and a  $6^-$  isomeric state [14] in  $^{138}\text{Cs}$  were reported from  $\beta$ -decay work. However, nothing has been reported for the high spin states of  $^{138}\text{Cs}$  ( $Z = 55$ ).

In the present work, we have identified the high spin states in  $^{138}\text{Cs}$  up to the 4626 keV level built on the  $6^-$  isomeric state and expanded the level scheme of  $^{137}\text{Cs}$ . Spins, parities, and configurations were assigned based on a comparison of the experimental energies and shell model calculations and level systematics, with good agreement between the theoretical and experimental values. The shell model calculations indicate the important role played by interactions between the excitation of the valence protons outside the  $Z = 50$  major shell and the  $f_{7/2}$  valence neutron outside the  $N = 82$  major shell.

## II. EXPERIMENTAL RESULTS

The measurements reported in the present work were carried out at Lawrence Berkeley National Laboratory with the Gammasphere detector array. The array consisted of 102 Compton suppressed Ge detectors. A spontaneously fissioning  $^{252}\text{Cf}$  source of strength  $\approx 62 \mu\text{Ci}$  was sandwiched between two Fe foils of thickness  $10 \text{ mg/cm}^2$ . This was mounted in a 7.62 cm diameter plastic (CH) ball to absorb  $\beta$  rays and conversion electrons. A total of  $5.7 \times 10^{11}$  triple and higher fold coincidence events were collected. The coincidence data were analyzed with the RADWARE software package [15].

### A. Identification of $^{138}\text{Cs}$

More than 100 nuclei are populated in the spontaneous fission of  $^{252}\text{Cf}$ , and many transitions from different nuclei

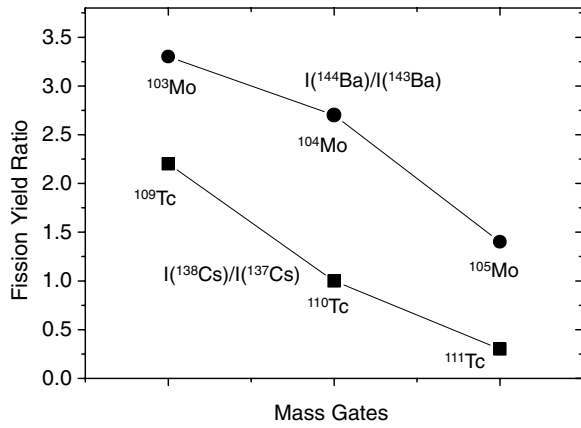


FIG. 1. Fission yield ratios of  $^{138}\text{Cs}$  and  $^{137}\text{Cs}$  in  $^{109,110,111}\text{Tc}$  gates,  $^{144}\text{Ba}$  and  $^{143}\text{Ba}$  in  $^{103,104,105}\text{Mo}$  gates [20].

overlap even in the coincidence spectra. Furthermore, there are always multiple pairs of correlated partners for a given nucleus. By gating on known  $\gamma$  rays in different partner isotopes, we can identify the transitions of interest in a particular nucleus. The fission partners of the  $^{138}\text{Cs}$  nucleus are  $^{109}\text{Tc}$  ( $5n$ ),  $^{110}\text{Tc}$  ( $4n$ ), and  $^{111}\text{Tc}$  ( $3n$ ). The level schemes of  $^{109,110,111}\text{Tc}$  were reported by our group [16,17] and by Urban *et al.* [18]. A number of low spin (1,2) levels up to 2500 keV built on the ground state were reported by Carlson *et al.* [13] from  $\beta$  decay of  $^{138}\text{Xe}$ . A  $6^-$  isomeric state in  $^{138}\text{Cs}$  was reported by Carraz *et al.* [14].

With the above-mentioned Tc identifications achieved, we searched for high spin states and transitions in  $^{138}\text{Cs}$ . By gating on known transitions in  $^{109,110,111}\text{Tc}$  isotopes, we identified a 1156.9 keV transition, which we assigned to  $^{138}\text{Cs}$ . In  $^{109,110,111}\text{Tc}$  gates, the yield ratios of the 1156.9 keV transition in  $^{138}\text{Cs}$  and the 1184.7 keV transition in  $^{137}\text{Cs}$  were measured to be 2.2, 1.1, and 0.3, as shown in Fig. 1. The variations of

these ratios follow those of  $^{144}\text{Ba}$  and  $^{143}\text{Ba}$  in  $^{103,104,105}\text{Mo}$  gates [20], to support the proposition that the 1156.9 keV transition belongs to  $^{138}\text{Cs}$ . The fact that the ratios are smaller than those observed in Ba-Mo pairs also suggests that the 1156.9 keV transition is not directly feeding the isomeric state or the ground state.

To show how we identified other transitions that belong to  $^{138}\text{Cs}$ , several triple-coincidence spectra were generated by gating on the 1156.9 keV transition in  $^{138}\text{Cs}$  and transitions in its partner Tc isotopes. A spectrum double gating on the 1156.9 keV transition in  $^{138}\text{Cs}$  and the 137.3 keV transition in  $^{109}\text{Tc}$  is shown in Fig 2(a). The coincident  $\gamma$ -ray transitions in both  $^{138}\text{Cs}$  and  $^{109}\text{Tc}$  were clearly identified. In Fig. 2(b), a spectrum double gating on the 1156.9 and 174.5 keV transitions in  $^{138}\text{Cs}$  is shown. The coincident transitions of  $^{138}\text{Cs}$  and its Tc partners are indicated. Extensive cross-checking with many other triple-coincidence spectra led to identifications and placements of the transitions in  $^{138}\text{Cs}$ . We have observed a total of 15 new transitions and placed them into the level scheme with 13 new levels, as shown in Fig. 3.

The level scheme of  $^{138}\text{Cs}$  established in the present work is shown in Fig. 3. Excited levels are observed to be populated up to  $\approx 4.63$  MeV in  $^{138}\text{Cs}$ . The ground state and  $6^-$  isomeric state in  $^{138}\text{Cs}$  were reported in Refs. [13] and [14], respectively. For the neighboring  $N = 83$  isotone,  $^{136}\text{I}$  ( $Z = 53$ ), Urban *et al.* [10] reported the  $1^-$  ground state and a  $6^-$  isomeric state. Compared with the level scheme of  $^{136}\text{I}$ , it is most likely that the observed yrast cascade of  $^{138}\text{Cs}$  in the present work is built on the 79.9 keV  $6^-$  isomeric state. This is supported by the fact that spontaneous fission populates high spin states. Based on the decay patterns, the levels are arranged into different bands. Table I shows the transition energies and relative intensities of all the transitions identified in  $^{138}\text{Cs}$ .

The total internal conversion coefficients ( $\alpha_{\text{total}}$ ) were measured to determine the multiplicities of the low

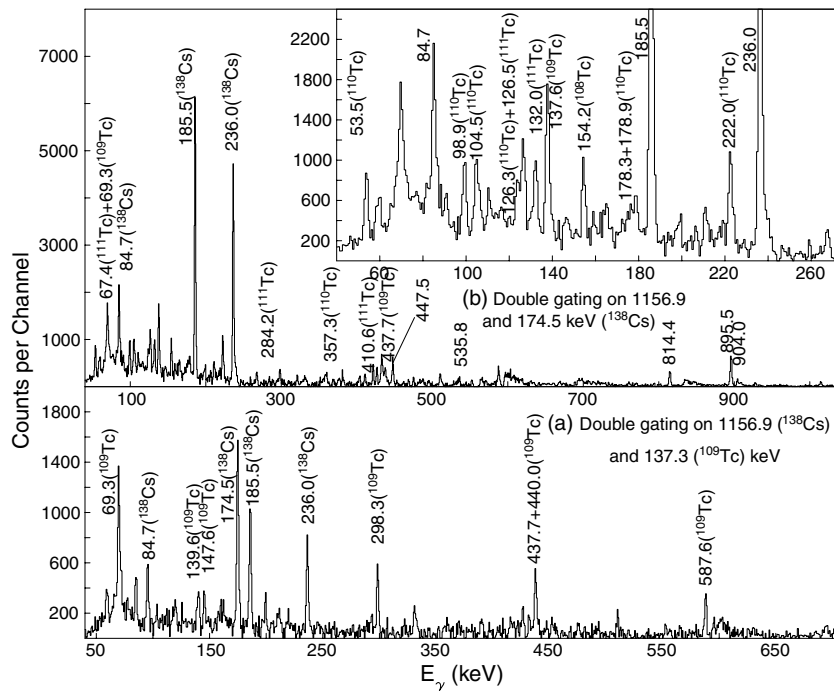


FIG. 2. (a) Spectrum gating on 1156.9 keV transition in  $^{138}\text{Cs}$  and 137.3 keV transition in  $^{109}\text{Tc}$ , (b) spectrum gating on 1156.9 and 174.5 keV transitions in  $^{138}\text{Cs}$ .

TABLE I. Energies and relative intensities determined for transitions in  $^{138}\text{Cs}$ .

$E_\gamma$ (keV)	$I_\gamma$	$E_i$ (keV)	$E_f$ (keV)
84.7	32.9	1917.5	1832.9
174.5	100	254.4	79.9
185.5	52.5	1596.8	1411.3
236.0	40.3	1832.8	1596.8
320.7	2.2	1917.5	1596.8
421.5	5.9	1832.8	1411.3
426.4	2.6	3158.3	2731.9
447.5	8.2	3260.5	2813.0
461.6	0.9	4626.1	4164.5
535.8	2.0	3348.8	2813.0
814.4	5.2	2731.9	1917.5
895.5	16.0	2813.0	1917.5
904.0	3.5	4164.5	3348.8
909.8	1.2	4258.6	3348.8
1156.9	77	1411.3	254.4

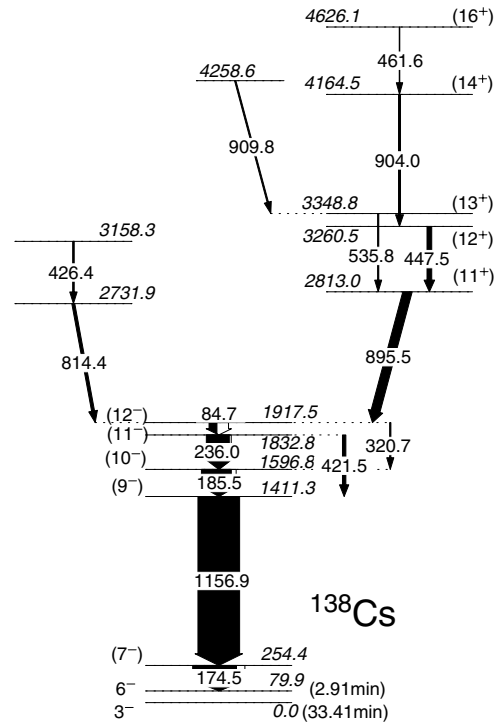
energy transitions. The  $\alpha_{\text{total}}$  of low energy transitions can be determined from the intensity balance in and out of a state by double gating on two transitions in the same cascade. The total internal conversion of two low energy transitions, 185.5 and 84.7 keV, were measured. For the 185.5 keV transition, the  $\alpha_{\text{total}}$  was measured by double gating on the 1156.9 and 84.7 keV transitions. In this gate, the difference in relative  $\gamma$ -ray intensities of the 185.5 and 236.0 keV transitions is equal to the conversion electron intensity. The  $\alpha_{\text{total}}$  of the 84.7 keV transition was measured by double gating on 185.5 and 895.5 keV transitions. Their total internal conversion coefficients were determined to be  $\alpha_{\text{total}}(84.7 \text{ keV}) = 1.39 \pm 0.22$  and  $\alpha_{\text{total}}(185.5 \text{ keV}) = 0.18 \pm 0.04$ . The theoretical values were calculated as  $\alpha_{(\text{total}, E_2)}(185.5 \text{ keV}) = 0.22$ ,  $\alpha_{(\text{total}, M_1)}(185.5 \text{ keV}) = 0.16$ ,  $\alpha_{(\text{total}, E_2)}(84.7 \text{ keV}) = 3.42$ ,  $\alpha_{(\text{total}, M_1)}(84.7 \text{ keV}) = 1.48$  [2]. Comparing with the theoretical values, their multipolarities were deduced as pure  $M1$  for the 84.7 keV transition,  $M1$  and/or  $E2$  for the 185.5 keV transition.

### B. Level scheme of $^{137}\text{Cs}$

The level scheme of  $^{137}\text{Cs}$  was reported by Broda *et al.* [19] from a deep inelastic one-proton-transfer reaction. From our fission data, we confirmed the level scheme of  $^{137}\text{Cs}$  with more transitions and levels identified. We observed seven new transitions and placed them into the level scheme with five new levels. An example of the coincidence spectrum for  $^{137}\text{Cs}$  obtained by double gating on 1184.7 and 487.1 keV transitions is shown in Fig. 4. The transitions in  $^{137}\text{Cs}$  and its fission partners can be clearly identified. The level scheme of  $^{137}\text{Cs}$  constructed in the present work is shown in Fig. 5.

### III. SHELL MODEL CALCULATIONS AND SPIN, PARITY, AND CONFIGURATION ASSIGNMENTS

The spin, parity, and configuration assignments for  $^{137}\text{Cs}$  and  $^{138}\text{Cs}$  were essentially based on comparisons

FIG. 3. Partial level scheme of  $^{138}\text{Cs}$ . Energies are in keV.

of the experimental level energies with those of the shell model calculations. In these calculations, we assumed  $^{132}\text{Sn}$  to be a closed core and let the valence protons occupy the five single-particle (SP) orbits of the 50–82 shell, while for the neutrons, the model space included the six orbits of the 82–126 shell. We employed a shell model Hamiltonian with the single-particle energies taken from experiment and the two-body effective interaction derived from the CD-Bonn free nucleon-nucleon potential [21]. The same Hamiltonian was used in recent studies of  $^{134}\text{Sn}$ ,  $^{134}\text{Sb}$ , and  $^{135}\text{Sb}$ , producing very good results [22–24]. The values of the proton and neutron SP energies as well as a brief discussion of the derivation of the effective interaction can be found in Ref. [24]. Comparisons of the experimental level energies with the shell model calculations for  $^{137}\text{Cs}$  and  $^{138}\text{Cs}$  are shown in Tables II and III, respectively.

#### A. $^{137}\text{Cs}$

As shown in Table II, the newly observed 3168.1, 4117.6, 4291.0, 3303.6, and 3503.4 keV levels are assigned a  $J^\pi$  of  $(19/2^+)$ ,  $(19/2^+)$ ,  $(21/2^+)$ ,  $(19/2^-)$ , and  $(21/2^-)$ , respectively. The unassigned 4351.6 keV and 4776.9 keV levels in Ref. [19] (confirmed in the present work) are assigned a  $J^\pi$  of  $(23/2^+)$  and  $(25/2^+)$ , respectively.

The configuration assignments of levels for  $^{137}\text{Cs}$  previously reported in [19] are confirmed in the present work with good overall agreement between theory and experiment, as shown in Table II. The 3303.6 keV  $(19/2^-)$  and 3503.4 keV  $(21/2^-)$  levels are both assigned as  $\pi g_{7/2}^4 h_{11/2}$  and the 3168.1 keV  $(19/2^+)$  level as  $\pi g_{7/2}^3 d_{5/2}^2$ . The last four experimental levels of Table II, 4117.6 keV  $(19/2^+)$ , 4291.0 keV

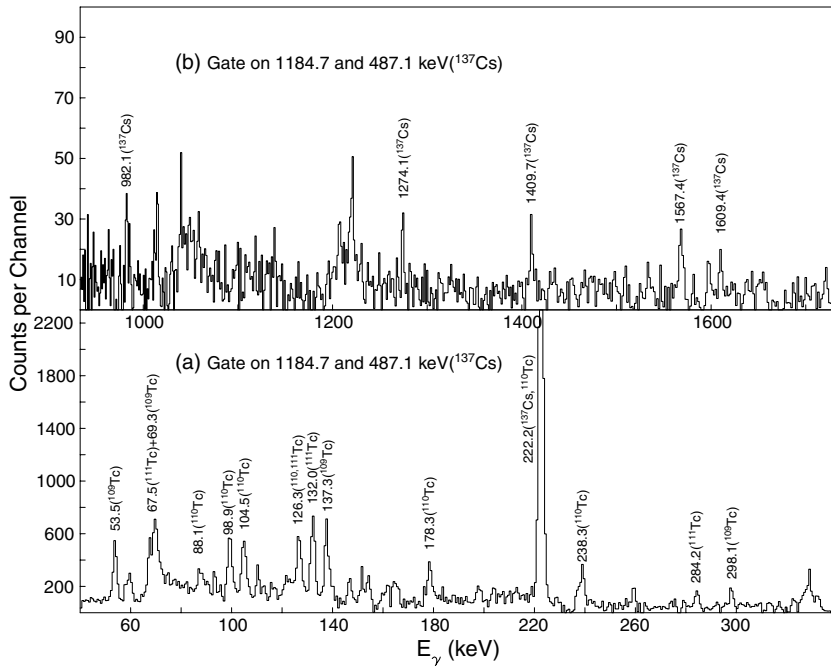


FIG. 4. Spectra gating on 1184.7 and 487.1 keV transitions in  $^{137}\text{Cs}$ , showing (a) the low energy region and (b) the high energy region.

( $21/2^+$ ), 4351.6 keV ( $23/2^+$ ), and 4776.9 keV ( $25/2^+$ ) levels have no theoretical counterparts. They are most probably related to particle-hole neutron excitations of the  $^{132}\text{Sn}$  core. We suggest a configuration of  $\pi g_{7/2}^5 \nu f_{7/2} h_{11/2}^{-1}$  for these levels (see Fig. 5) since this excitation has been identified in the isotope  $^{135}\text{I}$  ( $Z = 53$ ) and confirmed by theory [5,25]. The neutron particle-hole  $\nu f_{7/2} h_{11/2}^{-1}$  configurations are not described within our model space.

### B. $^{138}\text{Cs}$

The level scheme of  $^{138}\text{Cs}$  is built on the isomeric state at 79.9 keV which has been assigned  $6^-$  [14]. The spins, parities, and dominant configurations are assigned by comparing the experimental level energies with the calculated ones, which

are given in Table III. The levels in  $^{138}\text{Cs}$  can be interpreted by coupling an  $f_{7/2}$  neutron to the levels in  $^{137}\text{Cs}$ . Based on the shell model calculations and the above-mentioned multipolarity determinations of low energy transitions, ( $7^-$ ), ( $9^-$ ), ( $10^-$ ), ( $11^-$ ) and ( $12^-$ ) are assigned to the 254.4, 1411.3, 1596.8, 1832.8, and 1917.5 keV levels, respectively. Note that a ( $7^-$ ) state and a low energy transition from ( $7^-$ ) to ( $6^-$ ) were also reported in the neighboring  $N = 83$  isotope,  $^{136}\text{I}$ , by Urban *et al.* [10]. In  $^{138}\text{Cs}$ , positive-parity levels should occur above the 1917.5 keV ( $12^-$ ) level related to coupling an  $f_{7/2}$

TABLE II. Comparison of experimental ( $E_{\text{ex}}$ ) and calculated ( $E_{\text{th}}$ ) level energies (in MeV) of  $^{137}\text{Cs}$ , and deviations between them.

$I^\pi$	$E_{\text{ex}}$	$E_{\text{th}}$	$\Delta = E_{\text{th}} - E_{\text{ex}}$	Leading component
$7/2^+$	0.00	0.00	0.00	$\pi g_{7/2}^5$
$(11/2^+)$	1.18	1.35	0.17	$\pi g_{7/2}^5$
$(15/2^+)$	1.67	1.68	0.01	$\pi g_{7/2}^5$
$(17/2^+)$	1.89	2.02	0.13	$\pi g_{7/2}^4 d_{5/2}$
$(21/2^+)$	2.78	3.01	0.23	$\pi g_{7/2}^4 d_{5/2}$
$(19/2^+)$	2.88	3.07	0.19	$\pi g_{7/2}^4 d_{5/2}$
$(19/2^+)$	3.17	3.51	0.34	$\pi g_{7/2}^3 d_{5/2}^2$
$(23/2^+)$	3.47	3.75	0.28	$\pi g_{7/2}^3 d_{11/2}^2$
$(19/2^-)$	3.30	3.29	-0.01	$\pi g_{7/2}^4 h_{11/2}$
$(23/2^-)$	3.50	3.40	-0.10	$\pi g_{7/2}^4 h_{11/2}$
$(21/2^-)$	3.50	3.40	-0.10	$\pi g_{7/2}^4 h_{11/2}$
$(27/2^-)$	4.41	4.40	-0.01	$\pi g_{7/2}^4 h_{11/2}$
$(29/2^-)$	5.02	5.22	0.20	$\pi g_{7/2}^3 d_{5/2}^2 h_{11/2}$
$(31/2^-)$	5.50	5.36	-0.14	$\pi g_{7/2}^3 d_{5/2}^2 h_{11/2}$
$(19/2^+)$	4.12			$\pi g_{7/2}^5 \nu f_{7/2} h_{11/2}^{-1}$
$(21/2^+)$	4.29			$\pi g_{7/2}^5 \nu f_{7/2} h_{11/2}^{-1}$
$(23/2^+)$	4.35			$\pi g_{7/2}^5 \nu f_{7/2} h_{11/2}^{-1}$
$(25/2^+)$	4.78			$\pi g_{7/2}^5 \nu f_{7/2} h_{11/2}^{-1}$

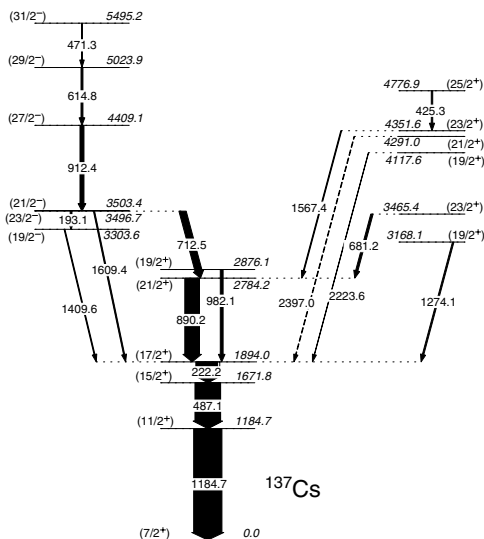


FIG. 5. Partial level scheme of  $^{137}\text{Cs}$ . Energies are in keV.

neutron to the proton  $g_{7/2} \rightarrow h_{11/2}$  and  $(g_{7/2})^2 \rightarrow d_{5/2}h_{11/2}$  negative-parity excitations found in  $^{137}\text{Cs}$ . By considering the corresponding couplings,  $(11^+)$ ,  $(12^+)$ ,  $(13^+)$ ,  $(14^+)$ , and  $(16^+)$  are tentatively assigned to the 2813.0, 3260.5, 3348.8, 4164.5, and 4626.1 keV levels, respectively.

The angular correlation coefficients  $A_2^{\text{ex}}$  and  $A_4^{\text{ex}}$  for the 174.5 and 1156.9 keV cascade were measured to be  $-0.07(1)$  and  $-0.02(2)$ , as described in Ref. [26]. They are consistent with the theoretical coefficients of  $A_2^{\text{th}} = -0.071$  and  $A_4^{\text{th}} = 0.0$  [27], for pure quadrupole and pure dipole transitions and for the proposed spin assignments of  $(9^-)$  and  $(7^-)$  to the 1411.3 and 254.4 keV levels. This measurement also indicates that the 174.5 keV transition has  $M1$  character, while the 1156.9 keV transitions has  $E2$  character.

It can be seen in Table III that in  $^{138}\text{Cs}$ , the coupling between the  $g_{7/2}$  valence protons and the  $f_{7/2}$  neutron,  $\pi g_{7/2}^5 \nu f_{7/2}$ , is assigned to the first three excitations, 79.9 keV  $(6^-)$ , 254.4 keV  $(7^-)$ , and 1411.3 keV  $(9^-)$ . The  $g_{7/2} \rightarrow d_{5/2}$  excitation,  $\pi g_{7/2}^4 d_{5/2} \nu f_{7/2}$ , is assigned to the 1596.8 keV  $(10^-)$ , 1832.8 keV  $(11^-)$ , and 1917.5 keV  $(12^-)$  levels. The coupling of the  $f_{7/2}$  neutron with the  $g_{7/2} \rightarrow h_{11/2}$  excitation, fits well the 2813.0 keV  $(11^+)$ , 3260.5 keV  $(12^+)$ , and 3348.8 keV  $(13^+)$  levels. The 4164.5 keV  $(14^+)$  and 4626.1 keV  $(16^+)$  levels are interpreted with a  $\pi g_{7/2}^3 d_{5/2} h_{11/2} \nu f_{7/2}$  configuration.

The shell model calculations indicate an important role played by the coupling of the odd protons outside the  $Z = 50$  closed shell and the  $f_{7/2}$  neutron outside the  $N = 82$  closed shell. Also note in Table III that the configuration mixing in  $^{138}\text{Cs}$  is extensive. We show only the leading components and their percentages of the total theoretical wave function.

#### IV. DISCUSSION

Figure 6 shows the yrast excitations of Cs isotopes near the  $N = 82$  major shell closure. The level spacings exhibit strong shell effects of the  $N = 82$  neutron major shell. The level schemes of  $^{140,142}\text{Cs}$  are not included, since the spins and parities of their yrast states are not available.

TABLE III. Same as Table II, but for  $^{138}\text{Cs}$ , relative to the  $6^-$  state.

$I^\pi$	$E_{\text{ex}}$	$E_{\text{th}}$	$\Delta = E_{\text{th}} - E_{\text{ex}}$	Leading component	Percentage
$6^-$	0.0	0.0	0	$\pi g_{7/2}^5 \nu f_{7/2}$	46
$7^-$	0.17	0.15	-0.02	$\pi g_{7/2}^5 \nu f_{7/2}$	41
$9^-$	1.33	1.55	0.22	$\pi g_{7/2}^5 \nu f_{7/2}$	51
$10^-$	1.52	1.75	0.23	$\pi g_{7/2}^4 d_{5/2} \nu f_{7/2}$	80
$11^-$	1.75	1.89	0.14	$\pi g_{7/2}^4 d_{5/2} \nu f_{7/2}$	57
$12^-$	1.84	1.98	0.14	$\pi g_{7/2}^4 d_{5/2} \nu f_{7/2}$	77
$11^+$	2.73	2.79	0.06	$\pi g_{7/2}^4 h_{11/2} \nu f_{7/2}$	61
$12^+$	3.18	3.25	0.07	$\pi g_{7/2}^4 h_{11/2} \nu f_{7/2}$	61
$13^+$	3.27	3.33	0.06	$\pi g_{7/2}^4 h_{11/2} \nu f_{7/2}$	63
$14^+$	4.08	3.80	-0.28	$\pi g_{7/2}^3 d_{5/2} h_{11/2} \nu f_{7/2}$	81
$16^+$	4.55	4.63	0.08	$\pi g_{7/2}^3 d_{5/2} h_{11/2} \nu f_{7/2}$	79

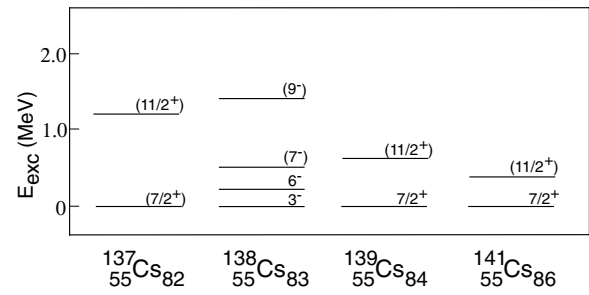


FIG. 6. Yrast states of Cs isotopes. Data from Refs. [28,29] and this work.

Figure 7 shows the yrast excitations of the  $N = 82$  and  $N = 83$  isotones with a few valence protons outside the  $Z = 50$  major shell closure. A similarity is seen in the yrast level patterns between  $^{137}\text{Cs}$  ( $Z = 55$ ) and its neighboring  $N = 82$  isotone  $^{135}\text{I}$  ( $Z = 53$ ) [25]. For the  $N = 83$  isotones  $^{138}\text{Cs}$  and  $^{136}\text{I}$  [6,9,10], a similar cascade pattern is observed. However, one more yrast state, the  $10^-$  state, is identified in  $^{138}\text{Cs}$  but not reported in  $^{136}\text{I}$ . For the  $^{136}\text{I}$  nucleus, the 47s  $6^-$  isomeric state was assigned a configuration of  $\pi g_{7/2}^2 d_{5/2} \nu f_{7/2}$  by Urban *et al* [10]. The assignment was supported by shell model calculations of the SMPN(400) set of two-body matrix, in which the position of the  $\pi d_{5/2}$  orbital was lowered by 400 keV. In our shell model calculations of  $^{138}\text{Cs}$ , we predict a yrast  $6^-$  state in  $^{138}\text{Cs}$  arising from the  $\pi g_{7/2}^5 \nu f_{7/2}$  configuration, while a second  $6^-$  state predicted at 185 keV higher is dominated by the  $\pi g_{7/2}^4 d_{5/2} \nu f_{7/2}$  configuration. When we similarly lower the  $\pi d_{5/2}$  orbital energy, we observe a reordering of the two  $6^-$  states. However, the level ordering of the  $9^-$ ,  $10^-$ ,  $11^-$ ,  $12^-$  levels change too, resulting in significant disagreement between the calculated and experimental level energies. Based on this disagreement, we assigned the  $6^-$  state in  $^{138}\text{Cs}$  with a configuration of  $\pi g_{7/2}^5 \nu f_{7/2}$ . Note that our shell model calculations on  $^{136}\text{I}$  [30] predict the same  $\pi g_{7/2}^3 \nu f_{7/2}$  dominant configuration for the lowest  $6^-$  state and the existence of a  $10^-$  state at about the same energy as that calculated for  $^{138}\text{Cs}$ . Further studies are needed to verify these predictions.

The variations of the excitation energies of the  $11/2^+$  state in even- $N$  Cs isotopes versus the excitation energies of the first  $2^+$  state in the corresponding even-even Xe core are shown in Fig. 8. They change very rapidly in the region of  $N = 82$

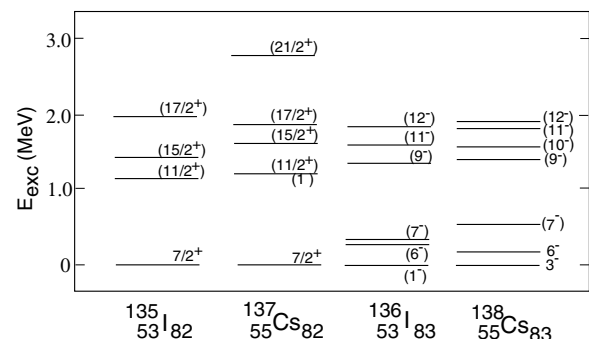


FIG. 7. Yrast states of  $N = 82$  and  $N = 83$  isotones.

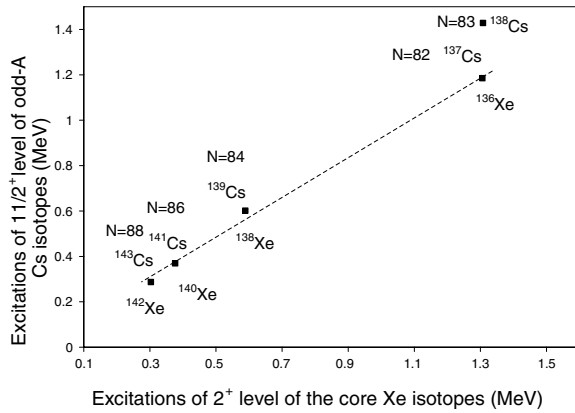


FIG. 8. Variations of excitation energies of the  $11/2^+$  states in the even- $aN$  Cs isotopes vs excitations of the first  $2^+$  state in the corresponding even-even Xe core.  $9^+$  state energy in  $^{138}\text{Cs}$  is also shown. Data are from Refs. [19,28,29] and from the present work.

major shell, with an almost linear relationship. The  $N = 83$  Cs isotone,  $^{138}\text{Cs}$ , is also shown in the figure by assuming that the  $9^-$  state can be attributed to the coupling between the lowest yrast excitation of the even-even core  $^{136}\text{Xe}$  with one  $g_{7/2}$  valence proton and one  $f_{7/2}$  valence neutron. For  $^{138}\text{Cs}$ , the coupling does not significantly reduce the excitation energy of the corresponding  $9^-$  state.

## V. CONCLUSION

In conclusion, the high spin states of the  $N = 83$  neutron-rich isotope  $^{138}\text{Cs}$  have been observed for the first time, and the level scheme of  $^{137}\text{Cs}$  expanded by observing the spontaneous fission of  $^{252}\text{Cf}$  with the Gammasphere. Shell model calculations were performed and used to interpret

the excitations in  $^{137,138}\text{Cs}$ . Note that these calculations are completely free from adjustable parameters. Spins, parities, and configurations were assigned to the levels of  $^{138}\text{Cs}$  based on total internal conversion coefficient measurements of the low energy transitions, shell model calculations, angular correlation measurements, and level systematics. Spin, parity, and configuration assignments for the newly observed levels in  $^{137}\text{Cs}$  were also made based on the shell model calculations. The level schemes of  $^{137,138}\text{Cs}$  established in the present work and the shell model calculations reveal significant contributions by the proton excitations in this important nuclear region near the doubly magic  $^{132}\text{Sn}$  nucleus. Similarities were observed between the  $N = 82$  isotones,  $^{137}\text{Cs}$  and  $^{135}\text{I}$ , as well as the  $N = 83$  isotones,  $^{138}\text{Cs}$  and  $^{136}\text{I}$ . The shell model calculations indicate the important role played by the coupling between the excitation of the fifth proton outside the  $Z = 50$  major shell and the  $f_{7/2}$  neutron outside the  $N = 82$  major shell.

## ACKNOWLEDGMENTS

The authors are indebted for the use of  $^{252}\text{Cf}$  to the Office of Basic Energy Sciences, U.S. Department of Energy, through the transplutonium element production facilities at the Oak Ridge National Laboratory. The authors would also like to acknowledge I. Ahmad, J. Greene, and R.V. F. Janssens for preparing the source. The work at Vanderbilt University, Lawrence Berkeley National Laboratory, and Lawrence Livermore National Laboratory is supported by the U.S. Department of Energy under Grant No. DE-FG05-88ER40407 and Contract Nos. DE-AC03-76SF00098 and W-7405-ENG48, respectively. The work at the University of Naples Federico II was supported in part by the Italian Ministero dell'Istruzione, dell'Università e della Ricerca (MIUR).

- 
- [1] J. Blomqvist, in *Proceedings of the 4th International Conference on Nuclei Far From Stability, Helsing, Denmark*, 1981, CERN 81-09 (unpublished), p. 536.
- [2] *Table of Isotopes*, 8th ed., edited by R. B. Firestone and V. S. Shirley (Wiley, New York, 1996).
- [3] H. Prade *et al.*, Nucl. Phys. **A472**, 381 (1987).
- [4] J. H. Hamilton *et al.*, Prog. Part. Nucl. Phys. **35**, 635 (1995).
- [5] C. T. Zhang *et al.*, Phys. Rev. Lett. **77**, 3743 (1996).
- [6] P. Bhattacharyya *et al.*, Phys. Rev. C **56**, R2363 (1997).
- [7] B. Fornal *et al.*, Phys. Rev. C **63**, 024322 (2001).
- [8] Y. X. Luo *et al.*, Phys. Rev. C **64**, 054306-1 (2001).
- [9] Y. X. Luo *et al.*, in *Fission and Properties of Neutron-Rich Nuclei: Proceedings of the 3rd International Conference, Sanibel Island, Florida, USA, November 2002*, edited by J. H. Hamilton, A. V. Ramayya, and H. K. Carter (World Scientific, Singapore, 2003), p. 310.
- [10] W. Urban *et al.*, Eur. Phys. J. A **27**, 257 (2006).
- [11] P. J. Daly *et al.*, Phys. Rev. C **59**, 3066 (1999).
- [12] J. K. Hwang *et al.*, Phys. Rev. C **69**, 057301 (2004).
- [13] G. H. Carlson *et al.*, Phys. Rev. C **9**, 283 (1974).
- [14] L. C. Carraz *et al.*, Nucl. Phys. **A171**, 209 (1971).
- [15] D. C. Radford, Nucl. Instrum. Methods Phys. Res. A **361**, 297 (1995).
- [16] Y. X. Luo *et al.*, Phys. Rev. C **70**, 044310 (2004).
- [17] Y. X. Luo *et al.*, Phys. Rev. C **74**, 024308 (2006).
- [18] W. Urban *et al.*, Eur. Phys. J. A **24**, 161 (2005).
- [19] R. Broda *et al.*, Phys. Rev. C **59**, 3071 (1998).
- [20] J. H. Hamilton *et al.*, Phys. Rep. **264**, 215 (1996).
- [21] R. Machleidt, Phys. Rev. C **63**, 024001 (2001).
- [22] A. Covello *et al.*, Prog. Part. Nucl. Phys. (to be published), available online at [www.sciencedirect.com](http://www.sciencedirect.com).
- [23] L. Coraggio, A. Covello, A. Gargano, and M. Itaco, Phys. Rev. C **73**, 031302(R) (2006).
- [24] L. Coraggio, A. Covello, A. Gargano, and M. Itaco, Phys. Rev. C **72**, 057302 (2005).
- [25] S. K. Saha *et al.*, Phys. Rev. C **65**, 017302 (2001).
- [26] A. V. Daniel *et al.*, Nucl. Instrum. Methods (to be published).
- [27] P. E. Haustein *et al.*, Nucl. Data Tables **10**, 321 (1972).
- [28] J. H. Hamilton *et al.* (unpublished).
- [29] A. Nowak *et al.*, Eur. Phys. J. A **6**, 1 (1999).
- [30] L. Coraggio, A. Covello, A. Gargano, and N. Itaco (unpublished).